

Effect of retardation on the frequency and linewidth of plasma resonances in a two-dimensional disk of electron gas

I. V. Zagorodnev,^{1,*} D. A. Rodionov^{1,2} and A. A. Zabolotnykh¹

¹*Kotelnikov Institute of Radioengineering and Electronics of Russian Academy of Sciences, Moscow, 125009, Russia*

²*Moscow Institute of Physics and Technology, Dolgoprudny, Moscow Region, 141701, Russia*

 (Received 11 September 2020; revised 22 March 2021; accepted 7 May 2021; published 21 May 2021)

We theoretically analyze dominant plasma modes in a two-dimensional disk of electron gas by calculating the absorption of an incident electromagnetic wave. The problem is solved in a self-consistent approximation, taking into account electromagnetic retardation effects. We use the Drude model to describe the conductivity of the system. The absorption spectrum exhibits a series of peaks corresponding to the excitation of plasma waves. The position and linewidth of the peaks designating, respectively, the frequency and damping rate of the plasma modes. We estimate the influence of retardation effects on the frequency and linewidth of the fundamental (dipole) and axisymmetric (quadrupole) plasma modes both numerically and analytically. We find the net damping rate of the modes to be dependent on not only the sum of the radiative and collisional decays but also their intermixture, even for small retardation. We show that the net damping rate can be noticeably less than that determined by collisions alone.

DOI: [10.1103/PhysRevB.103.195431](https://doi.org/10.1103/PhysRevB.103.195431)

I. INTRODUCTION

Plasma waves or plasmons in two-dimensional (2D) electron systems (ESs) were first discovered more than 40 years ago [1–4]. Recognized as one of the basic and easily excited collective oscillations, they have presently become a widely used platform for active fundamental and applied research, with considerable application potential in the fields of plasmonics, nanophotonics, and optoelectronics [5–10]. The interaction of plasmons with electromagnetic radiation is used ubiquitously to various studies in these areas.

Given an infinite homogeneous 2DES in a vacuum environment, the dispersion of plasma waves was defined in [11] as

$$q^2 = \frac{\omega^2}{c^2} + \left(\frac{\omega^2}{2\pi n e^2 / m} \right)^2, \quad (1)$$

where n and m are the electron concentration and effective mass, q is the plasmon wave vector, and c is the speed of light in vacuum (note that we use the CGS units throughout the presented analysis). The derivation of Eq. (1) is based on the assumption of infinite electron relaxation time. The dispersion law that follows from Eq. (1) is restricted to the region “below” the light cone $\omega = cq$. For this reason, the excitation of plasmons with electromagnetic radiation requires introduction of an inhomogeneity into the 2DES or external field. Therefore, metallic gratings [2,5,9,12,13], near-field optical microscopy [6,14–16], or samples with confined geometries, e.g., disks or strips [17–20], are utilized. The 2D disk, in particular, is one of the simplest configurations for both manufacturing and theoretical analysis—fabricated without metallic electrodes, such a system is perfectly suitable for

making a more direct comparison between the experimental data and theoretical calculations.

Plasmons in conductive 2D disks have been studied since 1985 [21–25], and most recently, they have been intently discussed with regard to graphene structures [16,26,27]. However, most of this work has been concerned with the quasiolestatic (quasistatic) or nonretarded regime, when the size of the sample is much smaller than the wavelength of the electromagnetic radiation. Retardation effects, on the other hand, significantly alter the properties of plasma oscillations, even in an infinite system [28–30]. Thus, in a disk-shaped 2DES retardation affects plasmon spectra, drastically reduces the plasmon damping rate, and considerably increases the quality factor [31–35]. At the same time, taking into account retardation effects greatly complicates the analytical treatment of plasma modes, which might explain the prevalent use of a numerical approach in this case [36–41]. In the presented paper we demonstrate the feasibility of qualitative and in some instances even quantitative analysis that accounts for the retardation effects.

In a disk-shaped 2DES, the eigenplasma modes are characterized by the radial number $n_r = 1, 2, 3, \dots$ and the orbital (angular) momentum number $l = 0, \pm 1, \pm 2, \dots$ [21,22,31,37]. The $l = 0$ mode corresponds to the axisymmetric oscillations where the charges and currents move exclusively in the radial direction. This mode is also called dark (or breathing) mode since it has a zero dipole moment, and therefore interacts rather weakly with electromagnetic radiation [33,42]. By contrast, in the $l = 1$ mode, the currents flow through the center as well as along the edge of the disk. The frequency of this mode is lower compared to the axisymmetric mode.

To estimate the frequency of plasma resonances in a finite-size sample, it is common to apply the phenomenological

*zagorodnev@phystech.edu

“quantization rule” of plasmon wave vector q in dispersion law (1). For example, according to the rule in a disk-shaped 2DES with the radius R , the fundamental mode ($l = 1$, $n_r = 1$) in the quasistatic regime is well described by $q \approx 1.1/R$. This approximation is sufficiently accurate for calculating the plasmon frequency and even the damping rate when electromagnetic retardation effects are neglected. However, taking the retardation into consideration results in an additional contribution to the net plasmon damping rate due to electromagnetic radiation. This contribution is not described by the dispersion law (1) as in the derivation of it only nonradiative (localized near 2DES) modes were considered. Consequently, the overall damping rate of the plasmon resonances in finite-size 2DESs cannot be fully described by a simple quantization rule of the plasmon wave vector.

In this paper, motivated by recent experiments [33–35], we analyze the frequency and damping rate of the plasma modes in a 2D disk for angular momentum $l = 0$ and $l = 1$ by calculating the absorption power of an electromagnetic wave. First, we transform the Maxwell’s equations into an integro-differential equation for the current density. Then we expand the unknown components of the current density in a Taylor-like series in a sense of the Galerkin method. Cutting the series we find the current density approximately. Finally, we determine the dependence of the frequency and linewidth of the absorption peaks on a retardation parameter. The absorption maxima indicate the excitation of plasma waves.

The two factors affecting the linewidth are the collisional (or dissipative) decay rate inversely proportional to the electron relaxation time and radiative decay rate related to the emission of electromagnetic radiation. Although most often the linewidth is assumed to represent purely additive effects of these two kinds of damping [43–46], we find that the linewidth is not merely the sum of these two decays. It contains additional mixing contributions. To the best of our knowledge, such intermixture of the plasmon dampings have been discussed for the first time. Furthermore, we obtain some analytical approximations for the frequency and damping rate of the plasma modes with $l = 0$ and $l = 1$ excited in a 2D disk.

In the following sections of the paper we introduce the essential equations along with solution methods (Sec. II), expand on the specifics of the axisymmetric (Sec. III) and fundamental modes (Sec. IV), and close with discussion and conclusions (Sec. V).

II. KEY EQUATIONS

Consider a 2D electron-gas disk of radius R in vacuum in the plane $z = 0$. Let $\mathbf{r} = (x, y)$ be the radius vector in the disk plane. Following the approach in Refs. [47,48], we seek the system response to an incident external electric field $\mathbf{E}^{\text{ext}}(\mathbf{r})e^{-i\omega t}$ with oscillation frequency ω . The total electric field $\mathbf{E}^{\text{tot}}(\mathbf{r})e^{-i\omega t}$ represents the superposition of the external field and the field induced by electron density in disk $\mathbf{E}^{\text{ind}}(\mathbf{r})e^{-i\omega t}$. According to the theory of linear response, the current density in the disk becomes

$$\mathbf{j}(\mathbf{r}) = \sigma(\omega)\mathbf{E}^{\text{tot}}(\mathbf{r}) = \sigma(\omega)[\mathbf{E}^{\text{ext}}(\mathbf{r}) + \mathbf{E}^{\text{ind}}(\mathbf{r})]. \quad (2)$$

We consider Drude model for conductivity $\sigma(\omega) = ne^2\tau/m(1 - i\omega\tau)$, where n , m , and τ are the 2D concentration, effective mass, and carriers relaxation time, respectively. We assume that equilibrium carrier concentration is homogeneous (i.e., “hard wall” confining potential).

In fact, the Drude conductivity is governed by only two independent parameters, intrinsic to the system—the collisional damping rate $\gamma = 1/\tau$ and ne^2/m , with the frequency ω being an extraneous parameter from the standpoint of the dynamical response. The internal properties can be varied nearly independently, even within a single sample, for example, by changing the temperature or carrier concentration [49]. In the case of restricted systems, the size of the system becomes an additional parameter. However, it is convenient to introduce the following dimensionless parameters:

$$\tilde{\gamma} = \frac{\gamma R}{c} = \frac{R}{c\tau}, \quad \tilde{\Gamma} = \frac{2\pi ne^2 R}{mc^2}. \quad (3)$$

It will be shown that these very parameters determine the characteristics of plasma waves in a disk. We refer to $\tilde{\Gamma}$ as the retardation parameter. Notice that the sum of these parameters (without R/c factor) define the absorption line broadening in an infinite 2DES in the presence of magnetic field [32,50].

Based on Eqs. (3), the conductivity can be rewritten in terms of the dimensionless parameters as

$$\sigma(\tilde{\omega}) = i \frac{c}{2\pi} \frac{\tilde{\Gamma}}{\tilde{\omega} + i\tilde{\gamma}}, \quad (4)$$

where $\tilde{\omega} = \omega R/c = 2\pi R/\lambda$ is the dimensionless frequency, which is equal to the ratio of the disk perimeter to the wavelength λ of the external radiation. Here the case of $\tilde{\omega} \ll 1$ corresponds to the quasistatic regime. In the following analysis we focus mainly on the dependence of plasmon characteristics on the retardation parameter $\tilde{\Gamma}$ for any values of $\tilde{\omega}$.

In a practical sense, considering standard high-mobility GaAs/AlGaAs quantum wells with typical 2D electron concentration $n \sim 10^{11} \text{ cm}^{-2}$, for the radius of disk-shaped samples of up to 1.2 cm, the retardation parameter $\tilde{\Gamma}$ can reach the value of 10 [34], whereas the dimensionless relaxation rate $\tilde{\gamma}$ is less than or on the order of unity.

Mathematical analysis of plasmons poses quite a challenge since the relationship between the current density and the induced electric field is nonlocal. For the self-consistent derivation of the electric field induced in a disk we first consider the corresponding electrostatic $\varphi(\mathbf{r}, z, t)$ and vector $\mathbf{A}(\mathbf{r}, z, t)$ potentials described by Maxwell’s equations in the Cartesian coordinate system, in CGS units:

$$\Delta \mathbf{A}(\mathbf{r}, z, t) - \frac{1}{c^2} \frac{\partial^2}{\partial t^2} \mathbf{A}(\mathbf{r}, z, t) = -\frac{4\pi}{c} \mathbf{j}(\mathbf{r}, t) \delta(z), \quad (5)$$

$$\Delta \varphi(\mathbf{r}, z, t) - \frac{1}{c^2} \frac{\partial^2}{\partial t^2} \varphi(\mathbf{r}, z, t) = -4\pi \rho(\mathbf{r}, t) \delta(z). \quad (6)$$

Here c is the speed of light, $\rho(\mathbf{r}, t)$ and $\mathbf{j}(\mathbf{r}, t)$ are, respectively, the charge density and density of current, and Δ is the three-dimensional Laplace operator.

The above equations are derived in the Lorenz gauge

$$\frac{1}{c} \frac{\partial}{\partial t} \varphi(\mathbf{r}, z, t) + \text{div} \mathbf{A}(\mathbf{r}, z, t) = 0. \quad (7)$$

Given the cylindrical symmetry, the system can be characterized by the angular momentum l and radial number n_r . Hence, using the cylindrical coordinates (r, θ, z) , we can express the vector quantity under consideration in terms of their radial $A_r(r, \theta, z, t) = A_x \cos \theta + A_y \sin \theta$ and azimuthal $A_\theta(r, \theta, z, t) = -A_x \sin \theta + A_y \cos \theta$ components, with $A_z(\mathbf{r}, t) = 0$ —as there are no current sources to contribute to the z component of the vector potential. Then, applying the Fourier transformation with respect to time, i.e., considering the solutions of the form $\exp(i l \theta - i \omega t)$, we reformulate the Maxwell's equations as follows:

$$\begin{pmatrix} \square_l - \frac{1}{r^2} & -\frac{2il}{r^2} \\ \frac{2il}{r^2} & \square_l - \frac{1}{r^2} \end{pmatrix} \mathbf{A}(r, z) = -\frac{4\pi}{c} \mathbf{j}(r) \delta(z), \quad (8)$$

where $\square_l = \frac{\omega^2}{c^2} + \frac{\partial^2}{\partial r^2} + \frac{1}{r} \frac{\partial}{\partial r} + \frac{\partial^2}{\partial z^2} - \frac{l^2}{r^2}$ is the time and angle Fourier transform of the d'Alembert operator in the cylindrical coordinates $\mathbf{A}(r, z) = [A_r(r, z), A_\theta(r, z)]^T$ and $\mathbf{j}(r) = [j_r(r), j_\theta(r)]^T$. As a next step, the scalar potential φ is ex-

pressed through the vector potential from the Lorenz gauge in (7). Thus, using the transformation

$$\mathbf{A}(r, z) = S \mathbf{A}_S(r, z), \quad S = \begin{pmatrix} i & -i \\ 1 & 1 \end{pmatrix}. \quad (9)$$

we diagonalize the system in (8) to obtain

$$\begin{pmatrix} \square_{l+1} & 0 \\ 0 & \square_{l-1} \end{pmatrix} \mathbf{A}_S(r, z) = -\frac{4\pi}{c} \mathbf{j}_S(r) \delta(z). \quad (10)$$

Then, taking the Hankel transform of the result, we express the transformed vector potential through the transformed current. Then, applying the inverse Hankel transform and inverse transformation S , we find the vector potential in the disk plane to be

$$\mathbf{A}(r, 0) = \frac{2\pi}{c} \int_0^R G_l(r, r') \mathbf{j}(r') r' dr', \quad (11)$$

with the following kernel:

$$G_l(r, r') = \int_0^\infty \frac{p dp}{\beta} S \begin{pmatrix} J_{l+1}(pr') J_{l+1}(pr) & 0 \\ 0 & J_{l-1}(pr') J_{l-1}(pr) \end{pmatrix} S^{-1}. \quad (12)$$

Here, at $p < \omega/c$, we choose the branch of the square root relation $\beta = \sqrt{p^2 - \omega^2/c^2}$ with the negative imaginary part since it corresponds to the waves outgoing from the disk.

After that we determine the induced electric field in the disk plane $z = 0$,

$$\mathbf{E}^{\text{ind}}(r) = i \frac{c}{\omega} \left[\hat{D} + \frac{\omega^2}{c^2} \right] \mathbf{A}(r, 0), \quad (13)$$

where

$$\hat{D} = \begin{pmatrix} \frac{1}{r} \frac{d}{dr} r \frac{d}{dr} - \frac{1}{r^2} & i l \frac{d}{dr} \frac{1}{r} \\ \frac{i l}{r^2} \frac{d}{dr} r & -\frac{l^2}{r^2} \end{pmatrix}. \quad (14)$$

This is merely a composition of the gradient and divergence operators grad div in the polar coordinate (without z components). Substituting Eq. (11) into (13), we finally derive the relationship between the current density and the induced electric field:

$$\mathbf{E}^{\text{ind}}(r) = i \frac{2\pi}{\omega} \left(\frac{\omega^2}{c^2} + \hat{D} \right) \int_0^R G_l(r, r') \mathbf{j}(r') r' dr'. \quad (15)$$

Once the dimensionless coordinate r/R is introduced, the electric field in Eq. (15) is governed solely by $\tilde{\omega}$ —the dimensionless frequency.

Importantly, the kernel $G_l(r, r')$ has parity $(-1)^{l+1}$ with respect to the (formal) transformation $r \rightarrow -r$ since its defining Bessel functions of order $l \pm 1$ have parity $(-1)^{l+1}$. As the parity is preserved by the differential operator \hat{D} in Eq. (14), the induced field, and therefore the current density, can be odd and even functions for $l = 0$ and $l = 1$, respectively.

Now let us consider the behavior of the current density at the center and at the edge of the disk. The normal to the edge component of the current should vanish at the edge, i.e., $j_r(R) = 0$. At the center of the disk the behavior is far more

complex. Given the continuity equation

$$-i\omega\rho(r) + \frac{dj_r(r)}{dr} + \frac{j_r(r) + ilj_\theta(r)}{r} = 0, \quad (16)$$

the current density relation at the center of the disk becomes

$$j_r(0) + ilj_\theta(0) = 0, \quad (17)$$

assuming there are no singularities in charge density and derivative of the current density. For the axisymmetric mode, it immediately leads to $j_r(0) = 0$. For $l \neq 0$ further Taylor series expansion of the current density about $r = 0$ results in an extra condition $2j_r'(0) + ilj_\theta'(0) = 0$ (with the prime denoting the derivatives with respect to r), which ensures zero charge at the center of the disk.

To calculate the response of the disk on an external electric field, one should solve Eqs. (2) and (15) with the above mentioned boundary conditions. However, obtaining the exact solution to these equations is virtually unachievable. Therefore, to find an approximate solution, we expand the unknown vector-function $\mathbf{j}(r)$ in a complete set of basis functions, integrate the system over r , and then reduce it to a matrix equation on the expanding coefficients. After that, we truncate the matrix to retain only the dominant terms. Finally, by solving the resultant matrix equation, we calculate the expansion coefficients and, consequently, the desired current density, which determines the response of the system. The accuracy of this procedure can be assessed by the successive increase of the number of basis functions.

Although any complete set of functions can be chosen, it is most appropriate to consider functions that are analytically integrable with the kernel (12) of the integral equation (15). Fortunately, any power function is a suitable choice since it can be integrated analytically with respect to the coordinates r, r' at least with the inner kernel of the integral operator $G_l(r, r')$ (however, the integral over the parameter p of the

Hankel transform is retained for some cases). Also, it is worth noting that due to the kernel properties, the current $\mathbf{j}(r)$ has parity $(-1)^{l+1}$. All the characteristics mentioned above constitute the key mathematical features that permit the exact calculation of most given integrals, yielding analytical expressions for the current density and related plasma characteristics.

Having determined the current density in the system, we calculate the absorption power

$$P(\omega) = \int_0^R \frac{1}{2} \operatorname{Re}(\mathbf{j}^* \cdot \mathbf{E}^{\text{tot}}) 2\pi r dr = \frac{\pi\gamma}{2\Gamma} \int_0^R |\mathbf{j}|^2 r dr, \quad (18)$$

which provides us with information about the position and width of the plasma resonances.

III. AXISYMMETRIC MODE ($l = 0$)

A. Numerical solution

For the axisymmetric mode the azimuthal components of the current and induced electric field are absent. Using the properties of the derivatives of the Bessel functions of the first order, which determine the kernel $G_0(r, r')$, the expression for the induced electric field can be reduced to

$$E_r^{\text{ind}}(r) = \frac{2\pi i}{\omega} \int_0^\infty \beta J_1(pr) F(p) p dp, \quad (19)$$

where $J_1(x)$ is the Bessel function of the first kind, $\beta = \sqrt{p^2 - \omega^2/c^2}$, and the auxiliary function $F(p) = \int_0^R j_r(r) J_1(pr) r dr$ is the Hankel transform of the current density $j_r(r)$. In the case $p < \omega/c$ the imaginary part of β becomes negative, indicating the waves outgoing from the disk.

To excite the axisymmetric mode, we choose the external electric field of the form

$$\mathbf{E}^{\text{ext}} = (E_r^{\text{ext}}, E_\theta^{\text{ext}})^T = E_0(1, 0)^T. \quad (20)$$

The exact origin of this kind of field is irrelevant to the main subject of this paper. It may arise from a multipole expansion of a complex field. For example, as a result of a decomposition of excitation field in near-field scanning optical microscopy, or of an oscillating dipole (or antenna) in the vicinity of the disk.

For the radial component of the current we apply the series expansion

$$j_r(r) = \sum_{n=1}^N \alpha_n \frac{r}{R} \left(1 - \frac{r^2}{R^2}\right)^n, \quad (21)$$

where α_n are unknown coefficients, and N is the number of basis functions under consideration. It is an odd power Taylor series that satisfies the boundary conditions. Unlike the basis functions chosen in Ref. [48] this one corresponds to parity of the kernel $G_l(r, r')$ and, besides, it gives more physical (smoother) dependence of charge density on the coordinate r in the vicinity of the disk center. The given basis set of functions can be orthonormalized, although we found it unnecessary. Comparing calculations results with those based on the orthonormal basis set (including all powers of r as well as only odd powers), we observe no significant differences.

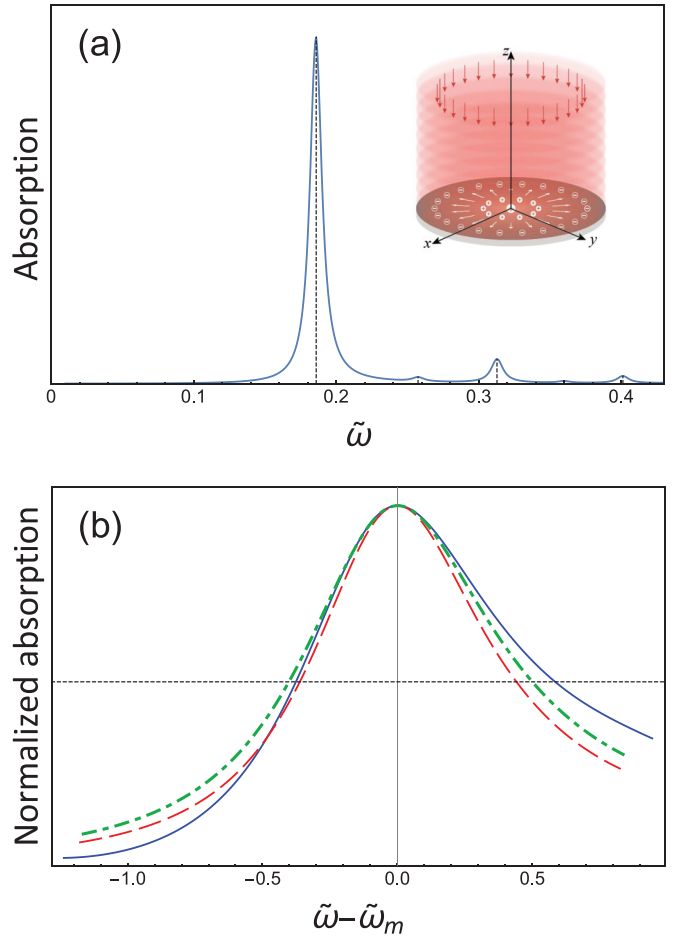


FIG. 1. (a) Dependence of the absorption power (in arbitrary units) of the axisymmetric plasma mode on the dimensionless frequency of the incident radiation $\tilde{\omega} = \omega R/c$, with R and c denoting the disk radius and the speed of light. Calculation results are carried out for the dimensionless collisional and retardation parameters $\tilde{\gamma} = \tilde{\Gamma} = 0.01$, which are determined by Eqs. (3). Plotted data indicate the first five resonances with $n_r = 1, 2, \dots, 5$. The inset schematically illustrates the excitation of the axisymmetric mode in the disk by external radiation. (b) Comparison of the main absorption maxima (with $n_r = 1$) for $\tilde{\gamma} = 1$ and different retardation parameter: $\tilde{\Gamma} = 0.5$ (solid line), $\tilde{\Gamma} = 2$ (dashed line), and $\tilde{\Gamma} = 4$ (dot-dashed line). The peaks are shifted on resonant frequency $\tilde{\omega}_m$ and are normalized in such a way that the absorption maximum equals unity. Ten terms of the current density expansion series in Eq. (21) were used for both figures.

To obtain the equation for coefficient α_n , we consecutively multiple Eq. (2) by k th basis function $(1 - r^2/R^2)^k r/R$ for $k = 1, 2, \dots, N$ and then integrate the result with the weight function r over the range $r \in [0, R]$. Here all integrals are calculated analytically (including the integral with respect to p). After that we arrive at a linear system of the unknown coefficients α_n , which is easy to solve. Thus, having determined the current density, we calculate the absorption power spectrum, according to Eq. (18), and analyze it.

For the purpose of illustration, Fig. 1 shows examples of the dependencies of the absorption power on the frequency of external radiation. Figure 1(a) was calculated for $\tilde{\gamma} = \tilde{\Gamma} =$

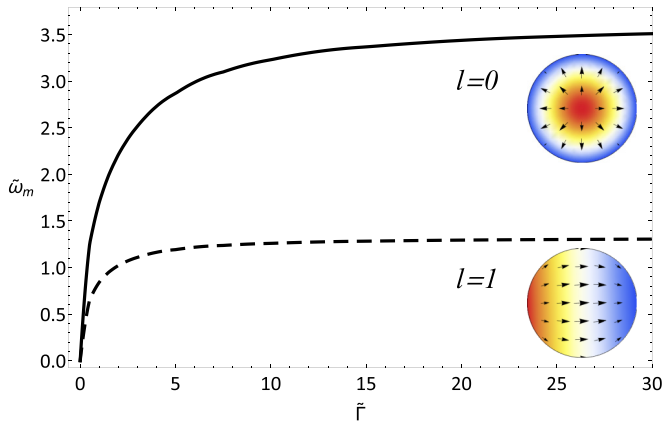


FIG. 2. Dependence of the dimensionless resonance frequency $\tilde{\omega}_m$ on the retardation parameter $\tilde{\Gamma}$ calculated for the plasma resonances of the radial number $n_r = 1$ and the orbital numbers $l = 0$ (solid curve) and $l = 1$ (dashed curve). Calculations are carried out using ten basis functions for the $l = 0$ mode and five basis functions for the $l = 1$ mode. Insets depict the charge and current distributions for the respective resonance modes.

0.01, i.e., in a quasistatic regime, with $\tilde{\omega} \ll 1$ (and $\tilde{\Gamma} \ll 1$), using the first ten basis functions. The data clearly indicate the first five resonances for $n_r = 1, 2, \dots, 5$, with more pronounced excitation of the mode with odd rather than even values of n_r . Also, the ratio of the resonant frequencies to that of the lowest ($n_r = 1$) resonance consistently comes to the value of $\sqrt{n_r}$ with a high degree of accuracy. Thus, it is evident that the phenomenological quantization rule of the 2D wave vector $q \approx 3.5n_r/R$ well describes the position of the resonances, at least for small damping.

Below we focus only on the main resonance with $n_r = 1$. From the dependence of the absorption power on the frequency we find the resonant frequency $\tilde{\omega}_m$ taken as a maximum of absorption as well as the linewidth $\Delta\tilde{\omega}$ taken as the full width at half-maximum. In general, they both depend on $\tilde{\gamma}$ and $\tilde{\Gamma}$. In a practical case of particular interest, $\tilde{\omega}_m \gg \tilde{\gamma}$, when the resonant peak is well resolved (i.e., the width of the peak is less than its position), the dependence of the resonant frequency on the retardation parameter is unique. This dependence is shown in Fig. 2. Thus, at small frequencies $\tilde{\omega}_m \approx 1.87\sqrt{\tilde{\Gamma}}$, which is consistent with Eq. (1) and the quantization rule $q \approx 3.5/R$ [21,31]. For large $\tilde{\Gamma}$, when the plasmon dispersion (1) approaches the dispersion of light $\omega = cq$, the resonant frequency tends to the asymptote $\tilde{\omega}_m \approx 3.5$, which likewise conforms to the given quantization rule.

The dependence of the linewidth on the retardation parameter is depicted in Fig. 3. In general, it depends on the ratio between the collisional and retardation parameters. In the case $\tilde{\gamma} = 0$, the linewidth clearly grows large with increasing $\tilde{\Gamma}$ reaching the asymptotic value about 2.3. However, at the finite collisional damping rate the linewidth actually decreases with increasing $\tilde{\Gamma}$ at small retardation. The narrowing of the peak is clearly visible in Fig. 1(b), in which normalized absorption spectra are shifted on resonant frequency for $\tilde{\Gamma} = 0.5, 2, 4$. Also, please see the lines marked by squares and diamonds in Fig. 3. In the following discussion we focus on this particular

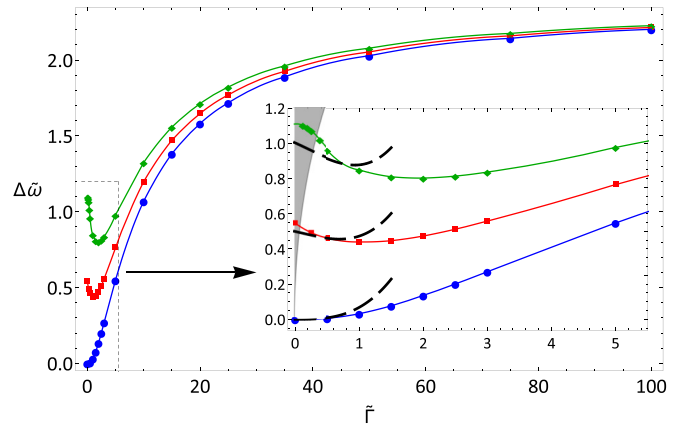


FIG. 3. Dependence of the dimensionless linewidth $\Delta\tilde{\omega} = \Delta\omega R/c$ on the retardation parameter $\tilde{\Gamma}$ calculated for the axisymmetric plasma resonance ($l = 0, n_r = 1$). Curves marked by (blue) circles, (red) squares, and (green) diamonds correspond to the dimensionless collisional damping $\tilde{\gamma} = 0, \tilde{\gamma} = 0.5$, and $\tilde{\gamma} = 1$, respectively. Calculations are based on the first ten terms in Eq. (21). The inset is a closeup of the data region of small retardation, with dashed lines showing the approximations from Eq. (27). The gray shaded area designates the overdamped region with strong plasmon damping, i.e., $\Delta\tilde{\omega} > \tilde{\omega}_m$.

case and find the approximation of the linewidth dependence on the retardation parameter. At small $\tilde{\Gamma}$ (at finite $\tilde{\gamma}$) the plasmon is overdamped. Although in the overdamped regime there still is weak resonance in the absorption spectra, it hardly can be associated with the plasma oscillations in the usual sense (there is no oscillations). Besides, the resonance is highly asymmetric with respect to frequency and it has a quality factor less unity. This regime is shown by gray shaded fill in Fig. 3.

B. Approximate solution

To begin with, we approximate the current distribution by a single basis function

$$j_r(r) = \alpha_1 \left(1 - \frac{r^2}{R^2}\right) \frac{r}{R}, \quad (22)$$

where α_1 is the only unknown coefficient. Then the Hankel transform of the current becomes $F(p) = 2\alpha_1 J_3(pR)/p^2$. Next, we substitute Eqs. (19), (20), and (22) into Eq. (2), multiply the resultant equation by $(1 - r^2/R^2)r^2/R$, and integrate the product over the radius. For this calculation we introduce the dimensionless coordinate r/R . After some algebraic manipulations, we arrive at

$$\alpha_1 = \frac{i24c\tilde{\Gamma}E_0}{15\pi \left[\tilde{\omega} + i\tilde{\gamma} - \frac{24\tilde{\Gamma}}{\tilde{\omega}} f(\tilde{\omega})\right]}, \quad (23)$$

where

$$f(\tilde{\omega}) = -\frac{16}{105\pi} + \frac{2H_3(2\tilde{\omega})}{\tilde{\omega}^4} + \frac{H_4(2\tilde{\omega})}{\tilde{\omega}^3} - i \frac{\tilde{\omega}^5 - 8\tilde{\omega}^3 + 48J_3(2\tilde{\omega}) + 24\tilde{\omega}J_4(2\tilde{\omega})}{24\tilde{\omega}^4}. \quad (24)$$

Here $H_n(x)$ is the Struve function.

Since the absorption power is proportional to $|\alpha_1|^2$, the resonance is determined by the minimum of the denominator of $|\alpha_1|$. In the limit $\tilde{\omega} \rightarrow 0$ we have

$$f(\tilde{\omega}) \rightarrow \frac{16}{35\pi} - \frac{64\tilde{\omega}^2}{2835\pi} - \frac{256\tilde{\omega}^4}{155925\pi} - \frac{i\tilde{\omega}^5}{4320} + \dots \quad (25)$$

Leaving only the first three terms in the expression (25) and neglecting the collisional damping, we determine the position of the absorption maximum $\tilde{\omega}_m$ for $\tilde{\Gamma} \ll 1$:

$$\tilde{\omega}_m^2 \approx 3.492\tilde{\Gamma}(1 - 0.172\tilde{\Gamma} - 0.01406\tilde{\Gamma}^2). \quad (26)$$

In the lowest order in $\tilde{\Gamma}$ (the quasistatic limit), this result perfectly matches the numerical solution and approximates that obtained earlier, with better than 1% accuracy [21,40].

At high $\tilde{\Gamma}$ the frequency approaches asymptotic value $\tilde{\omega}_m \approx 3.65$, which slightly differs from that obtained numerically. This means that one basis function is a good approximation at least for small $\tilde{\Gamma}$.

The linewidth of the absorption resonance $\Delta\tilde{\omega}$ is related to the imaginary part of the denominator of α_1 . Hence, using the last term in the Eq. (25) at $\tilde{\omega} = \tilde{\omega}_m$ we obtain

$$\Delta\tilde{\omega} \approx \tilde{\gamma} + 0.068\tilde{\Gamma}^3 + \tilde{\gamma}\tilde{\Gamma}(-0.172 - 0.058\tilde{\Gamma} + 0.04\tilde{\Gamma}^2). \quad (27)$$

Evidently the linewidth is comprised of three contributions: the collisional damping $\tilde{\gamma}$, the radiative damping $\propto \tilde{\Gamma}^3$, and the third term including the intermixture of $\tilde{\gamma}$ and $\tilde{\Gamma}$. Therefore, the resultant approximation (27) clearly demonstrates that the linewidth is not merely the sum of the collisional and radiative decays in contrast to Refs. [43–46]. As can be seen from the dashed curves in the inset to Fig. 3, the qualitative dependence of the linewidth on the retardation parameter is described relatively properly for small $\tilde{\Gamma}$. Indeed, retardation appears to affect the collisional linewidth $\tilde{\gamma}$ more dramatically than it follows from the approximate Eq. (27). In the next subsection we consider these contributing factors in detail to shed some light on the interplay of these parameters.

C. Qualitative description of the linewidth

In this part of the paper we give a physical explanation of established linewidth dependencies in connection with the properties of the disk plasma mode. Consider an external electric field exciting plasma oscillations at a resonant frequency defined in Eq. (26). Provided that energy losses over an oscillation period are small compared with the energy stored in the mode (i.e., far from the shaded region in Fig. 3), the (dimensional) linewidth $\Delta\omega$ can be determined as $\Delta\omega = P/W$, where P is the power loss averaged over the oscillation period and W is the energy stored in the plasma mode—electromagnetic energy and kinetic energy of the carriers [51]. Let us next find P and W for the current density specified in Eq. (22).

The net power loss can be treated as a sum of the losses associated with the Joule heating (caused by carrier collisions) P_J , and electromagnetic radiation P_{rad} . From the differential form of the Joule heating equation, we find

$$P_J = \frac{\text{Re}(\sigma^{-1})}{2} \int |j_r(r)|^2 2\pi r dr \approx \gamma \frac{\pi^2 R^3}{12c^2 \tilde{\Gamma}} |\alpha_1|^2. \quad (28)$$

At the same time, from the continuity Eq. (16), we determine the charge density at the resonance frequency: $\rho(r) = -i2\alpha_1[1 - 2(r/R)^2]/(\omega_m R)$. In this case, the electric and magnetic dipole moments are absent due to the symmetry of the charge and current distributions. At low frequency (small retardation), the radiation of the mode is defined by the electric quadrupole moment $Q = i\pi\alpha_1 R^3 \text{diag}\{1, 1, -2\}/(6\omega_m)$, where $\text{diag}\{\}$ is a diagonal matrix. Therefore, the radiative loss attributed to quadrupole radiation is given by

$$P_{\text{rad}} = \frac{|\ddot{Q}|^2}{180c^5} \approx 0.011 \frac{\pi^2 R^2 \tilde{\Gamma}^2}{c} |\alpha_1|^2. \quad (29)$$

The total energy W is the sum of the carrier kinetic energy W_k and the electromagnetic energy W_{em} . As long as losses are small, W can be calculated virtually at any point in time. However, it is somewhat easier to compute it at the moment of the peak current—in the absence of the charges and (non-radiating) electric fields. Hence, the kinetic energy can be formulated as

$$W_k = \frac{\pi}{\Gamma c} \int |j_r(r)|^2 2\pi r dr \approx \frac{\pi^2 R^3}{12\tilde{\Gamma} c^2} |\alpha_1|^2. \quad (30)$$

At the same exact moment, the electromagnetic energy is determined by the azimuthal component of the magnetic field H_θ . Thus, some algebraic manipulation yields

$$W_{\text{em}} = \int dV \frac{|H_\theta|^2}{8\pi} = \frac{\pi^2}{c^2} \int_{\frac{\omega}{c}}^{\infty} \frac{pdp}{\beta} |F(p)|^2 \approx \frac{\pi^2 R^3}{c^2} (0.014 + 0.0073\tilde{\Gamma} - 0.0063\tilde{\Gamma}^2). \quad (31)$$

In the given derivation process, we exclude the integration interval from 0 to ω/c as it corresponds to the emission of radiation, which leads to energy losses.

Finally, we find the linewidth as follows:

$$\Delta\tilde{\omega} \approx \tilde{\gamma} + 0.136\tilde{\Gamma}^3 + \tilde{\gamma}\tilde{\Gamma}(-0.172 - 0.058\tilde{\Gamma} + 0.1\tilde{\Gamma}^2). \quad (32)$$

It is the same approximation (27) up to second order of $\tilde{\Gamma}$. Difference in the third order of $\tilde{\Gamma}$ appear since in this section we evaluate the frequency of eigenmode with damping and treat emission of electromagnetic radiation as losses for eigenmode. In fact, it means that the frequency of the mode is complex and electromagnetic field increases with distance from the disk. While in the previous section we consider the response of disk on external radiation at real frequency, and therefore nongrowing fields with the increase of the distance from the disk.

In the lowest order in $\tilde{\Gamma}$, the electromagnetic energy radiation and radiative power loss can be neglected to yield $\Delta\omega = \gamma$. In the next order, the radiative power loss can still be ignored. However, the first term in the expansion of the electromagnetic energy in $\tilde{\Gamma}$ is a constant since any radial current produces circular magnetic fields above and below the disk, which contribute to the electromagnetic energy. Consequently, the linewidth is still proportional to γ , though it decreases with increasing the retardation parameter. In the succeeding orders in $\tilde{\Gamma}$, the radiative power loss must also be taken into account as it contributes to the overall damping. However, this effect is not very prominent being partially counteracted

by the growing denominator of W_{em} , as well as a stabilizing resonant frequency.

As follows from the derivation above, the approximation (32) behaves similarly to (27) and it is valid for a rather narrow range of parameters: $\tilde{\Gamma} \ll 1$ (the quasistatic limit) and $\tilde{\gamma} \ll \sqrt{\tilde{\Gamma}}$ (low damping). That is why the dashed curve in Fig. 3 does not well match the numerical solution for $\tilde{\gamma} = 1$.

So far we have demonstrated that the linewidth of the absorption peak relates to the plasmon damping, which is shown to be more than the mere sum of the collisional and radiative decay rates. As the denominator in Eq. (32) is found to depend on the retardation as well as radiative loss, it makes the overall dependence of the linewidth on the retardation parameter more complex, which can lead to substantial reduction in the total damping compared to the collisional decay rate γ .

IV. FUNDAMENTAL MODE ($l = 1$)

To excite the plasma mode with orbital number $l = 1$, we consider a circularly polarized electromagnetic plane wave

$$\begin{aligned}
 \mathbf{j}_1 &= 3\sqrt{\frac{3}{14}} \left[1 - \tilde{r}^2, \quad i \left(1 - \frac{\tilde{r}^2}{3} \right) \right]^T, & \mathbf{j}_2 &= 11\sqrt{\frac{5}{238}} \left[1 - \frac{81\tilde{r}^2 - 70\tilde{r}^4}{11}, \quad i \left(1 - \frac{27\tilde{r}^2 - 14\tilde{r}^4}{11} \right) \right]^T, \\
 \mathbf{j}_3 &= 23\sqrt{\frac{7}{1054}} \left[1 - \frac{378\tilde{r}^2 - 950\tilde{r}^4 + 595\tilde{r}^6}{23}, \quad i \left(1 - \frac{126\tilde{r}^2 - 190\tilde{r}^4 + 85\tilde{r}^6}{23} \right) \right]^T, \\
 \mathbf{j}_4 &= \frac{117}{7\sqrt{62}} \left[1 - \frac{370\tilde{r}^2 - 1750\tilde{r}^4 + 2695\tilde{r}^6 - 1302\tilde{r}^8}{13}, \quad i \left(1 - \frac{370\tilde{r}^2 - 1050\tilde{r}^4 + 1155\tilde{r}^6 - 434\tilde{r}^8}{39} \right) \right]^T, \\
 \mathbf{j}_5 &= \frac{59}{7}\sqrt{\frac{11}{142}} \left[1 - \frac{2565\tilde{r}^2 - 19250\tilde{r}^4 + 51940\tilde{r}^6 - 57834\tilde{r}^8 + 22638\tilde{r}^{10}}{59}, \right. \\
 &\quad \left. i \left(1 - \frac{855\tilde{r}^2 - 3850\tilde{r}^4 + 7420\tilde{r}^6 - 6426\tilde{r}^8 + 2058\tilde{r}^{10}}{59} \right) \right]^T,
 \end{aligned} \tag{33}$$

where $\tilde{r} = r/R$.

Repeating the procedure outlined in Sec. III A, we substitute the given current expansion into Eq. (2), consecutively multiply it by the basis functions and integrate over the disk area. Finally, solving the resultant system of equations for the coefficients C_n , we find the desired current density. Examples of the data calculated for the resonance with $n_r = 1$ and its linewidth are shown in Figs. 2 and 4, where the numerical calculations are carried out based on the first five basis functions.

To obtain analytical expressions for the frequency and linewidth of the fundamental resonance $n_r = 1$ at small $\tilde{\Gamma}$, we use only the first basis function from the set, similar to Sec. III B. We find the integral with respect to r and r' analytically, whereas that over the variable p we split into two parts—one integral from 0 to ω/c and the other from ω/c to ∞ . The former is evaluated approximately by expanding it to the third order of ω/c while the latter is evaluated analytically first, and then expanded to the third order of ω/c . Analyzing the obtained coefficient C_1 , we arrive at the approximate estimate of the resonant frequency

$$\tilde{\omega}_m \approx 1.07\sqrt{\tilde{\Gamma}}(1 - 0.293\tilde{\Gamma}), \tag{34}$$

incident normally onto the system, with the electric field in the plane of the disk given by $\mathbf{E}^{\text{ext}} = E_0(1, i)^T$. In this case we expand the current density in an orthonormal set of basis vector functions $\mathbf{j}(\mathbf{r}) = \sum C_n \mathbf{j}_n(\mathbf{r})$, with the scalar product $(\mathbf{j}_m(\mathbf{r}), \mathbf{j}_n(\mathbf{r})) = \int \mathbf{j}_m^*(\mathbf{r}) \cdot \mathbf{j}_n(\mathbf{r}) dS = \delta_{mn}$ [52,53], where the integral is taken over the disk area, and C_n are the expansion coefficients.

As follows from Sec. II, in the fundamental mode, the basis vector functions must be even with respect to the radius r for both components of the current density. For this reason we choose a polynomial sequence initiated with a quadratic function in r . However, it is not uniquely defined by the boundary conditions at the edge and center of the disk, as well as normalization. To eliminate the ambiguity, we consider the quasistatic regime of $\mathbf{j} \propto \text{grad } \varphi$, where φ is a scalar electric potential. Consequently, the components of the current density become interrelated as $j_\theta = i l \int j_r(r') dr' / r$. Applying this to the basis set and using the Gram-Schmidt orthonormalizing process, we arrive at the following functions:

and the linewidth

$$\Delta\tilde{\omega} \approx \tilde{\gamma} + 0.333\tilde{\Gamma}^2 + \tilde{\gamma}\tilde{\Gamma}(-0.586 + 0.150\tilde{\Gamma}). \tag{35}$$

In the quasistatic limit the frequency is again in a good agreement with that obtained earlier [21,40]. The qualitative difference between the linewidth of the modes with $l = 0$ and $l = 1$ is that the latter possesses a nonzero electric dipole moment. Therefore, the radiative power of the mode is proportional to $\tilde{\Gamma}$ and, as a result, in Eq. (35) there appears a $\tilde{\Gamma}^2$ term.

We again derive that the linewidth (35) is not merely the sum of the collisional and radiative decays and in general cannot be obtained by applying the phenomenological ‘‘quantization rule’’ to plasmon wave vector in a dispersion equation for plasma wave in infinite homogeneous 2DES [28,34]. Besides, it depends not only on the retardation parameter but also on the collisional decay rate in contrast to the proposal of Ref. [34]. However, detailed comparison between our calculations and the experiment [34] cannot be done accurately at the moment due to the following reasons: (i) the presence of dielectric substrate with high dielectric constant in real samples as well as metallic environment, and (ii) experimentally

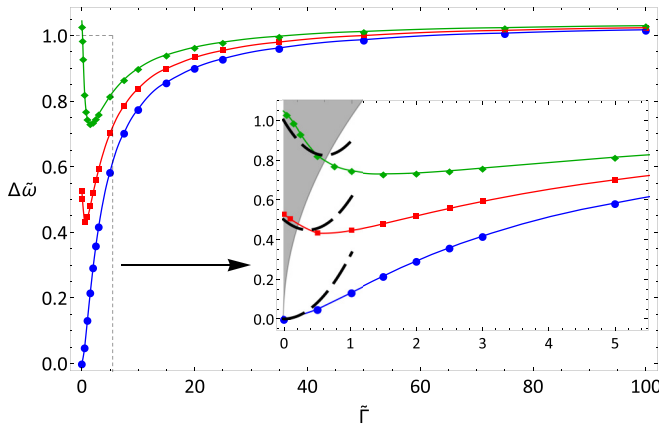


FIG. 4. Dependence of the dimensionless linewidth $\Delta\tilde{\omega}$ on the retardation parameter $\tilde{\Gamma}$ calculated for the fundamental resonance with $l = 1$, $n_r = 1$. Blue circle, red square, and green diamond correspond to $\tilde{\gamma} = 0$, $\tilde{\gamma} = 0.5$, and $\tilde{\gamma} = 1$, respectively. The inset is a closeup of the data region of small retardation, with dashed lines indicating the approximations from Eq. (35). The gray shaded area designates the overdamped region.

the resonance linewidth is determined from the dependence of luminescence intensity on magnetic field rather than on external radiation frequency (so far we have analyzed only the dependence on frequency).

At large $\tilde{\Gamma}$ we find that the frequency of the resonance $\tilde{\omega}_m$ approximately approaches asymptotic value 1.4, while the linewidth is slightly above 1.

V. DISCUSSION AND CONCLUSIONS

To make the analysis above more complete, we take into account the dielectric permittivity of the surrounding medium

ϵ by making the following replacement of the key parameters: $\tilde{\omega}_m \rightarrow \sqrt{\epsilon}\tilde{\omega}_m$, $\Delta\tilde{\omega} \rightarrow \sqrt{\epsilon}\Delta\tilde{\omega}$, and $\tilde{\gamma} \rightarrow \sqrt{\epsilon}\tilde{\gamma}$. As a result, we find that the broadening of the linewidth associated with the collisions does not change, while the radiative broadening decreases with increasing ϵ . It may additionally reduce the decay rate compared to γ .

In summary, we have studied numerically and analytically the fundamental (dipole) and axisymmetric (quadrupole) plasma modes in a 2D disk of electron gas taking into account retardation effects. We find that the frequency and the linewidth of the resonances can be fully described by two dimensionless parameters: $\tilde{\gamma}$ corresponding to the collisional damping rate, and the retardation parameter $\tilde{\Gamma}$ defined by Eq. (3). We establish that for weak collisions $\tilde{\gamma} \ll \tilde{\omega}$, the dimensionless frequency of plasma resonances $\tilde{\omega}$ is defined only by the retardation parameter $\tilde{\Gamma}$, as indicated by Eqs. (26) and (34). As for the resonance linewidth, we discover that it cannot be fully described by the sum of collisional ($\tilde{\gamma}$) and radiative ($\propto \tilde{\Gamma}^2$ for dipole and $\propto \tilde{\Gamma}^3$ for quadrupole modes) damping rates. The reason for such a complicated behavior of the linewidth is that with increasing retardation parameter, the radiation decay and the energy stored in the mode both grow simultaneously. The competition of these two processes leads to the nonmonotonous dependence of the linewidth on the retardation parameter, as well as the narrowing of the linewidth compared to collisional damping at small values of $\tilde{\Gamma}$, see Figs. 3 and 4.

ACKNOWLEDGMENTS

This work was carried out within the framework of the state task and supported by the Russian Foundation for Basic Research (Project No. 20-32-70188). We are grateful to V. M. Muravev, I. V. Kukushkin, and V. A. Volkov for valuable discussions.

- [1] C. C. Grimes and G. Adams, Observation of Two-Dimensional Plasmons and Electron-Ripplon Scattering in a Sheet of Electrons on Liquid Helium, *Phys. Rev. Lett.* **36**, 145 (1976).
- [2] S. J. Allen, D. C. Tsui, and R. A. Logan, Observation of the Two-Dimensional Plasmon in Silicon Inversion Layers, *Phys. Rev. Lett.* **38**, 980 (1977).
- [3] T. N. Theis, J. P. Kotthaus, and P. J. Stiles, Two-dimensional magnetoplasmon in the silicon inversion layer, *Solid State Commun.* **24**, 273 (1977).
- [4] D. C. Tsui, E. Gornik, and R. A. Logan, Far infrared emission from plasma oscillations of Si inversion layers, *Solid State Commun.* **35**, 875 (1980).
- [5] W. Knap, M. Dyakonov, D. Coquillat, F. Teppe, N. Dyakonova, J. Ąusakowski, K. Karpierz, M. Sakowicz, G. Valusis, D. Seliuta *et al.*, Field effect transistors for terahertz detection: Physics and first imaging applications, *J. Infrared Millim. Terahertz Waves* **30**, 1319 (2009).
- [6] A. N. Grigorenko, M. Polini, and K. S. Novoselov, Graphene plasmonics, *Nat. Photonics* **6**, 749 (2012).
- [7] P. Q. Liu, I. J. Luxmoore, S. A. Mikhailov, N. A. Savostianova, F. Valmorra, J. Faist, and G. R. Nash, Highly tunable hybrid metamaterials employing split-ring resonators strongly coupled to graphene surface plasmons, *Nat. Commun.* **6**, 8969 (2015).
- [8] D. A. Bandurin, D. Svinsov, I. Gayduchenko, S. G. Xu, A. Principi, M. Moskotin, I. Tretyakov, D. Yagodkin, S. Zhukov, T. Taniguchi *et al.*, Resonant terahertz detection using graphene plasmons, *Nat. Commun.* **9**, 5392 (2019).
- [9] A. Bylinkin, E. Titova, V. Mikheev, E. Zhukova, S. Zhukov, M. Belyanchikov, M. Kashchenko, A. Miakonkikh, and D. Svinsov, Tight-Binding Terahertz Plasmons in Chemical-Vapor-Deposited Graphene, *Phys. Rev. Appl.* **11**, 054017 (2019).
- [10] D. V. Fateev, K. V. Mashinsky, O. V. Polischuk, and V. V. Popov, Excitation of Propagating Plasmons in a Periodic Graphene Structure by Incident Terahertz Waves, *Phys. Rev. Appl.* **11**, 064002 (2019).
- [11] F. Stern, Polarizability of a Two-Dimensional Electron Gas, *Phys. Rev. Lett.* **18**, 546 (1967).
- [12] O. V. Polischuk, D. V. Fateev, T. Otsuji, and V. V. Popov, Plasmonic amplification of terahertz radiation in a periodic graphene structure with the carrier injection, *Appl. Phys. Lett.* **111**, 081110 (2017).

- [13] R. A. Maniyara, D. Rodrigo, R. Yu, J. Canet-Ferrer, D. S. Ghosh, R. Yongsunthon, D. E. Baker, A. Rezikyan, F. J. G. de Abajo, and V. Pruneri, Tunable plasmons in ultrathin metal films, *Nat. Photonics* **13**, 328 (2019).
- [14] Z. Fei, A. S. Rodin, G. O. Andreev, W. Bao, A. S. McLeod, M. Wagner, L. M. Zhang, Z. Zhao, M. Thiemens, G. Dominguez *et al.*, Gate-tuning of graphene plasmons revealed by infrared nano-imaging, *Nature (London)* **487**, 82 (2012).
- [15] J. Chen, M. Badioli, P. Alonso-González, S. Thongrattanasiri, F. Huth, J. Osmond, M. Spasenović, A. Centeno, A. Pesquera, P. Godignon *et al.*, Optical nano-imaging of gate-tunable graphene plasmons, *Nature (London)* **487**, 77 (2012).
- [16] A. Y. Nikitin, P. Alonso-González, S. Vélez, S. Mastel, A. Centeno, A. Pesquera, A. Zurutuza, F. Casanova, L. E. Hueso, F. H. L. Koppens *et al.*, Real-space mapping of tailored sheet and edge plasmons in graphene nanoresonators, *Nat. Photonics* **10**, 239 (2016).
- [17] V. M. Muravev, P. A. Gusikhin, I. V. Andreev, and I. V. Kukushkin, Novel Relativistic Plasma Excitations in a Gated Two-Dimensional Electron System, *Phys. Rev. Lett.* **114**, 106805 (2015).
- [18] V. M. Muravev, I. V. Andreev, S. I. Gubarev, V. N. Belyanin, and I. V. Kukushkin, Fine structure of cyclotron resonance in a two-dimensional electron system, *Phys. Rev. B* **93**, 041110(R) (2016).
- [19] V. M. Muravev, A. M. Zarezin, P. A. Gusikhin, A. V. Shupletsov, and I. V. Kukushkin, Proximity plasma excitations in disk and ring geometries, *Phys. Rev. B* **100**, 205405 (2019).
- [20] E. Nikulin, D. Mylnikov, D. Bandurin, and D. Svintsov, Edge diffraction, plasmon launching, and universal absorption enhancement in two-dimensional junctions, *Phys. Rev. B* **103**, 085306 (2021).
- [21] A. L. Fetter, Magnetoplasmons in a two-dimensional electron fluid: Disk geometry, *Phys. Rev. B* **33**, 5221 (1986).
- [22] D. C. Glattli, E. Y. Andrei, G. Deville, J. Poitrenaud, and F. I. B. Williams, Dynamical Hall Effect in a Two-Dimensional Classical Plasma, *Phys. Rev. Lett.* **54**, 1710 (1985).
- [23] R. P. Leavitt and J. W. Little, Absorption and emission of radiation by plasmons in two-dimensional electron-gas disks, *Phys. Rev. B* **34**, 2450 (1986).
- [24] V. Shikin, S. Nazin, D. Heitmann, and T. Demel, Dynamic response of quantum dots, *Phys. Rev. B* **43**, 11903 (1991).
- [25] Z. L. Ye and E. Zaremba, Magnetoplasma excitations in anharmonic electron dots, *Phys. Rev. B* **50**, 17217 (1994).
- [26] Z. Fang, S. Thongrattanasiri, A. Schlather, Z. Liu, L. Ma, Y. Wang, P. M. Ajayan, P. Nordlander, N. J. Halas, and F. J. G. de Abajo, Gated Tunability and Hybridization of Localized Plasmons in Nanostructured Graphene, *ACS Nano* **7**, 2388 (2013).
- [27] Z. Fang, Y. Wang, A. E. Schlather, Z. Liu, P. M. Ajayan, F. J. G. de Abajo, P. Nordlander, X. Zhu, and N. J. Halas, Active Tunable Absorption Enhancement with Graphene Nanodisk Arrays, *Nano Lett.* **14**, 299 (2014).
- [28] V. I. Fal'ko and D. E. Khmel'nitskii, What if a film conductivity exceeds the speed of light? *Zh. Eksp. Teor. Fiz.* **95**, 1988 (1989) [*Sov. Phys. JETP* **68**, 1150 (1989)].
- [29] A. O. Govorov and A. V. Chaplik, Retardation effects in the relaxation of a two-dimensional electron plasma, *Zh. Eksp. Teor. Fiz.* **95**, 1976 (1989) [*Sov. Phys. JETP* **68**, 1143 (1989)].
- [30] D. O. Oriekhov and L. S. Levitov, Plasmon resonances and tachyon ghost modes in highly conducting sheets, *Phys. Rev. B* **101**, 245136 (2020).
- [31] I. V. Kukushkin, J. H. Smet, S. A. Mikhailov, D. V. Kulakovskii, K. von Klitzing, and W. Wegscheider, Observation of Retardation Effects in the Spectrum of Two-Dimensional Plasmons, *Phys. Rev. Lett.* **90**, 156801 (2003).
- [32] S. A. Mikhailov, Microwave-induced magnetotransport phenomena in two-dimensional electron systems: Importance of electrodynamic effects, *Phys. Rev. B* **70**, 165311 (2004).
- [33] V. M. Muravev, I. V. Andreev, V. N. Belyanin, S. I. Gubarev, and I. V. Kukushkin, Observation of axisymmetric dark plasma excitations in a two-dimensional electron system, *Phys. Rev. B* **96**, 045421 (2017).
- [34] P. A. Gusikhin, V. M. Muravev, A. A. Zagitova, and I. V. Kukushkin, Drastic Reduction of Plasmon Damping in Two-Dimensional Electron Disks, *Phys. Rev. Lett.* **121**, 176804 (2018).
- [35] V. M. Muravev, I. V. Andreev, S. I. Gubarev, P. A. Gusikhin, and I. V. Kukushkin, Retardation Effects for "Dark" Plasma Modes in a Two-Dimensional Electron System, *JETP Lett.* **109**, 663 (2019).
- [36] M. I. Mishchenko, L. D. Travis, and A. A. Lacis, *Scattering, Absorption and Emission of Light by Small Particles* (Cambridge University Press, Cambridge, 2004).
- [37] M. V. Balaban, R. Sauleau, T. M. Benson, and A. I. Nosich, Dual Integral Equations Technique in Electromagnetic Wave Scattering by a Thin Disk, *Prog. Electromagn. Res. B* **16**, 107 (2009).
- [38] M. V. Balaban, O. V. Shapoval, and A. I. Nosich, THz wave scattering by a graphene strip and a disk in the free space: integral equation analysis and surface plasmon resonances, *J. Opt.* **15**, 114007 (2013).
- [39] J. Mäkitalo, M. Kauranen, and S. Suuriniemi, Modes and resonances of plasmonic scatterers, *Phys. Rev. B* **89**, 165429 (2014).
- [40] C. Forestiere, G. Gravina, G. Miano, M. Pascale, and R. Tricarico, Electromagnetic modes and resonances of two-dimensional bodies, *Phys. Rev. B* **99**, 155423 (2019).
- [41] C. Forestiere, G. Miano, and G. Rubinacci, Resonance frequency and radiative q-factor of plasmonic and dielectric modes of small objects, *Phys. Rev. Research* **2**, 043176 (2020).
- [42] F.-P. Schmidt, H. Ditlbacher, U. Hohenester, A. Hohenau, F. Hofer, and J. R. Krenn, Dark Plasmonic Breathing Modes in Silver Nanodisks, *Nano Lett.* **12**, 5780 (2012).
- [43] S. A. Mikhailov, Radiative decay of collective excitations in an array of quantum dots, *Phys. Rev. B* **54**, 10335 (1996).
- [44] I. Zoric, M. Zach, B. Kasemo, and C. Langhammer, Gold, platinum, and aluminum nanodisk plasmons: Material independence, subradiance, and damping mechanisms, *ACS nano* **5**, 2535 (2011).
- [45] I. V. Andreev, V. M. Muravev, V. N. Belyanin, and I. V. Kukushkin, Measurement of Cyclotron Resonance Relaxation Time in the Two-Dimensional Electron System, *Appl. Phys. Lett.* **105**, 202106 (2014).
- [46] I. V. Andreev, V. M. Muravev, V. N. Belyanin, and I. V. Kukushkin, Coherent and Incoherent Contributions to the Damping of Cyclotron Magnetoplasma Resonance for Two-Dimensional Electrons, *JETP Lett.* **102**, 821 (2015).

- [47] S. A. Mikhailov and N. A. Savostianova, Microwave response of a two-dimensional electron stripe, *Phys. Rev. B* **71**, 035320 (2005).
- [48] I. V. Zagorodnev, D. A. Rodionov, A. A. Zabolotnykh, and V. A. Volkov, Microwave absorption by axisymmetric plasmon mode in 2d electron disk, *Semiconductors* **53**, 1873 (2019).
- [49] I. V. Kukushkin, K. von Klitzing, K. Ploog, V. E. Kirpichev, and B. N. Shepel, Reduction of the electron density in GaAs-Al_xGa_{1-x} as single heterojunctions by continuous photoexcitation, *Phys. Rev. B* **40**, 4179 (1989).
- [50] K. Chiu, T. Lee, and J. Quinn, Infrared magneto-transmittance of a two-dimensional electron gas, *Surf. Sci.* **58**, 182 (1976).
- [51] X. Zheng, V. Volskiy, V. K. Valev, G. A. E. Vandenbosch, and V. V. Moshchalkov, Line position and quality factor of plasmonic resonances beyond the quasi-static limit: A full-wave eigenmode analysis route, *IEEE J. Sel. Top. Quantum Electron.* **19**, 4600908 (2013).
- [52] D. J. Bergman and D. Stroud, Theory of resonances in the electromagnetic scattering by macroscopic bodies, *Phys. Rev. B* **22**, 3527 (1980).
- [53] C. Forestiere and G. Miano, Material-independent modes for electromagnetic scattering, *Phys. Rev. B* **94**, 201406(R) (2016).